THE JOURNAL OF BIOLOGICAL CHEMISTRY VOL. 286, NO. 3, pp. 1836–1849, January 21, 2011

Inhibition of Proprotein Convertase SKI-1 Blocks Transcription of Key Extracellular Matrix Genes Regulating Osteoblastic Mineralization*

Received for publication, June 4, 2010, and in revised form, October 22, 2010 Published, JBC Papers in Press, November 12, 2010, DOI 10.1074/jbc.M110.151647

Jeff P. Gorski[‡1], Nichole T. Huffman[‡], Sridar Chittur[§], Ronald J. Midura[¶], Claudine Black[‡], Julie Oxford[‖], and Nabil G. Seidah[2]**

*From the [‡]Center of Excellence in the Study of Musculoskeletal and Dental Tissues and Department of Oral Biology, School of Dentistry, University of Missouri-Kansas City, Kansas City, Missouri 64108, the [§]Center for Functional Genomics, University at Albany, Rensselaer, New York 12144, the [¶]Department of Biomedical Engineering, Lerner Institute, Cleveland Clinic, Cleveland, Ohio 44195, the [‖]Department of Biology, Boise State University, Boise, Idaho 83725, and **Biochemical Neuroendocrinology, Institut de Recherches Cliniques de Montréal, Montréal, Québec, H2W 1R, Canada*

Mineralization, a characteristic phenotypic property of osteoblastic lineage cells, was blocked by 4-(2-aminoethyl) benzenesulfonyl fluoride hydrochloride (AEBSF) and decanoyl-Arg-Arg-Leu-Leu-chloromethyl ketone (dec-RRLL-cmk), inhibitors of SKI-1 (site 1; subtilisin kexin like-1) protease. Because SKI-1 is required for activation of SREBP and CREB (cAMP-response element-binding protein)/ATF family transcription factors, we tested the effect of these inhibitors on gene expression. AEBSF decreased expression of 140 genes by 1.5–3.0-fold including *Phex*, *Dmp1*, *COL1A1*, *COL11A1*, and fibronectin. Direct comparison of AEBSF and dec-RRLL-cmk, a more specific SKI-1 inhibitor, demonstrated that expression of *Phex*, *Dmp1*, *COL11A1*, and fibronectin was reduced by both, whereas *COL1A2* and *HMGCS1* were reduced only by AEBSF. AEBSF and dec-RRLL-cmk decreased the nuclear content of SKI-1-activated forms of transcription factors SREBP-1, SREBP-2, and OASIS. In contrast to AEBSF, the actions of dec-RRLL-cmk represent the sum of its direct actions on SKI-1 and indirect actions on caspase-3. Specifically, dec-RRLL-cmk reduced intracellular caspase-3 activity by blocking the formation of activated 19-kDa caspase-3. Conversely, overexpression of SKI-1-activated SREBP-1a and CREB-H in UMR106-01 osteoblastic cells increased the number of mineralized foci and altered their morphology to yield mineralization nodules, respectively. In summary, SKI-1 regulates the activation of transmembrane transcription factor precursors required for expression of key genes required for mineralization of osteoblastic cultures *in vitro* and bone formation *in vivo*. Our results indicate that the differentiated phenotype of osteoblastic cells and possibly osteocytes depends upon the non-apoptotic actions of SKI-1.

* This work was supported, in whole or in part, by National Institutes of Health Grant R01-052775 (NIAMS; to J. P. G.). This work was also supported by University of Missouri-Kansas City Center of Excellence for Mineralized Tissues and the University of Missouri Research Board (to J. P. G.).

[1] To whom correspondence should be addressed: Bone Biology Program, Center of Excellence in the Study of Musculoskeletal and Dental Tissues, Dept. of Oral Biology, School Of Dentistry, University of Missouri-Kansas City, 650 East 25th St., Kansas City, MO 64108. Tel.: 816-235-2537; Fax: 816-235-5524; E-mail: gorskij@umkc.edu.

[2] Supported by Canadian Institutes of Health Research TEAM Grant CTP 82946.

Bone formation and mineralization is a multistep process of differentiated osteoblastic cells. Based upon an analysis of gene expression during osteogenesis, Lian and Stein (1) noted that "peak levels of expressed genes reflect a developmental sequence of bone cell differentiation characterized by three principal periods: proliferation, extracellular matrix maturation, and mineralization, and two restriction points to which the cells can progress but cannot pass without further signals." These authors defined these three periods of osteoblastic differentiation in terms of patterns of sequential gene expression. For example, fibronectin and type I collagen expression denoted the pattern of pre-osteoblastic cells, alkaline phosphatase, and matrix GLA protein reflected the matrix maturation stage, and osteopontin and osteocalcin reflected the mineralization stage of mature osteoblastic cells (1). However, the number of genes required for normal bone formation and mineralization has grown rapidly to include Phex (*Phex*), dentin matrix protein1 (*Dmp1*), and type XI collagen (*COL11*).

Phex (phosphate-regulating endopeptidase homolog, X-linked) is a transmembrane metalloendoprotease enriched on bone osteoblasts and osteocytes (2). It is essential for phosphate homeostasis and bone mineralization as loss of function mutations result in X-linked hypophosphatemic rickets (3). Acidic phosphorylated dentin matrix protein 1 is highly expressed in teeth and osteocytes in bone. Mutations in *Dmp1* cause autosomal recessive hypophosphatemic rickets (4, 5). Elevated circulating levels of fibroblast growth factor 23 are a characteristic shared by both this human condition and by mice lacking Dmp1 (5). The hypophosphatemic rickets and elevated FGF23 (fibroblast growth factor 23) levels that occur in *Dmp1* null mice resemble the "hyp" mouse, which has an inactivating mutation in *Phex*. Because skeletal abnormalities in both these animal models can be largely but not completely rescued by feeding a high phosphate diet, DMP1 and Phex regulate an essential pathway controlling serum phosphate levels needed for mineralization of teeth and bone. Type XI collagen regulates the rate of fibrillogenesis of type I and II collagen and the ultimate size of fibrils (6). Homozygous *cho* mice containing a frameshift mutation in the COL11A1 gene die at birth with severe abnormalities of bone and tracheal

cartilage (7). In humans, COL11A1 mutations cause Marshall and Stickler syndromes (8) characterized by craniofacial abnormalities, nearsightedness, and hearing deficiencies. Finally, fibronectin is a multifunctional matrix-organizing protein possessing binding sites for collagen, glycosaminoglycan chains, and cell adhesion receptors. Blocking antibodies against the fibronectin receptor inhibit the mineralization of osteoblastic cells in culture (9–11). Although genetic knockouts and mutations causing skeletal abnormalities have identified these and other genes, detailed mechanisms controlling bone formation and mineralization are incompletely understood.

We have used osteoblastic culture models to investigate the mechanism controlling bone mineralization (12–18). Mineralization occurs within spherical, macromolecular, extracellular, vesicle-enriched complexes termed biomineralization foci. Because BMF[3] phosphoprotein biomarkers can be used to define areas of growing periosteum and developing fracture callus before their mineralization (14, 15), osteoblastic cultures appear to model bone formation *in vivo*. Proteomic analyses on laser micro-dissected mineralized BMF show they are enriched in phosphoproteins bone sialoprotein and BAG-75 and their fragments. Interestingly, both phosphoprotein cleavage and mineralization of BMF can be completely blocked with covalent serine protease inhibitor AEBSF, whereas 15 other inhibitors against acidic, metallo-, and sulfhydryl proteases were without effect (16). Based on these results, we hypothesized that initiation of bone mineralization is controlled by a serine protease. We recently showed that BMF contained an active, 105-kDa form of SKI-1 protease (18).

SKI-1 is a member of the proprotein convertase family (19). Proprotein convertases, serine proteases related to bacterial subtilisin and yeast kexin, cleave and activate growth factors, neuropeptides, toxins, glycoproteins, viral capsid proteins, and transcription factors. Transmembrane transcription factor precursors SREBP-1 and -2 are activated in a sequential process involving first SKI-1 cleavage and then site-2 protease cleavage (20). SREBPs can also be activated by caspase-3 (21, 22). The N-terminal fragments of SREBP-1 and SREBP-2 can then be imported into the nucleus where each regulates gene expression by binding to promoters containing consensus SRE sequences (23). Members of the CREB/ATF family of transcription factors (ATF-6, LUMAN (CREB3), OASIS/BBF2H7 (CREB3L2), CREB-H, CREB-4, and AIbZIP/Tisp40 (CREB3L4)) also require SKI-1-catalyzed activation. By activating ATF-6, SKI-1 serves as an initiator of the unfolded protein response, which decreases cellular stress by increasing chaperone production, influencing endoplasmic reticulum-associated degradation of proteins, and regulating membrane remodeling (24).

Recent studies indicate that SKI-1 is required for normal bone formation. First, the skeletons of mice deficient in OASIS (25) exhibit a severe osteopenia characterized by a type I collagen-deficient bone matrix and reduced osteoblastic activity (26). Second, mice overexpressing ICER (inducible cyclic AMP early repressor), a dominant negative effector of CREB/ATF transcription factors, displayed dramatically reduced trabecular bone and a reduced femoral bone formation rate (27). Third, SKI-1 is required for normal cartilage morphogenesis in zebrafish (28). Finally, conditional inactivation of SKI-1 in mice using a type II collagen CRE recombinase transgene leads to abnormal growth plate calcification (29). The purpose of this study was to determine whether SKI-1 protease controls initiation of osteoblastic mineralization.

EXPERIMENTAL PROCEDURES

Growth, Mineralization, and Treatment of UMR Cells with Protease Inhibitors—UMR106-01 bone sialoprotein cells were passaged and cultured as described previously (12). Cells were seeded at a density of 1.0×10^5 cells/cm^2 in growth medium. After 24 h, growth medium containing FBS was exchanged for 0.5% BSA (Millipore #82-045-1) containing medium. Sixty-four hours after plating, spent medium was exchanged with mineralization media (growth medium containing 0.1% BSA and 6.5 mM BGP). The addition of a supplemental phosphate source to UMR106-01 cultures prior to 64 h had no effect on the formation of mineral crystals.[4] Cultures were then incubated for up to an additional 24 h, at which time they were fixed with 70% ethanol.

In some experiments serine protease inhibitor AEBSF (EMD Biosciences, Inc.) or dec-RRLL-cmk (Bachem, Inc.) was added over a range of concentrations in mineralization media at 64 h after plating. We have shown previously (16) that 100 μM AEBSF is the minimum dosage able to effectively block mineralization of BMF within serum-depleted UMR cultures.

The extent of mineralization was either assessed visually by fluorescence microscopy (after staining with 10 μg/ml Alizarin red S dye) or quantitated by colorimetric calcium assay (17) by reference to a standard curve. In the latter case, calcium was first extracted from culture wells with acidified 70% ethanol, and the extracts were then concentrated before analysis. Transgenic DMP1 GFP mice were kindly provided by Drs. I. Kalajzic and D. W. Rowe, University of Connecticut Health Center.

SDS Gel Electrophoresis and Western Blotting—Protein samples were electrophoresed under reducing conditions on 4–20% linear gradient gels (Pierce/Thermo Scientific) according to Laemmli (30) and electroblotted onto PVDF membranes (Millipore Corp.) for 1.5–2 h at 100 V in 10 mM CAPS buffer (pH 11.0) containing 10% methanol. Blots were processed with primary antibody and horseradish peroxidase-conjugated secondary antibody as described previously (17),

[3] The abbreviations used are: BMF, biomineralization foci; SKI-1, site-1 or subtilisin/kexin isoenzyme-1; BGP, β-glycerol phosphate; SRE, sterol response element; SREBP, SRE binding transcription factor; BAG-75, bone acidic glycoprotein-75; AEBSF, 4-(2-aminoethyl) benzenesulfonyl fluoride hydrochloride; MTT, 3-(4,5-dimethylthiazol-2-yl)-2,5-diphenyltetrazolium bromide; Z-DEVD-OPH, benzyloxycarbonyl- Asp-Glu-Val-Asp-[2,6-difluorophenoxy]-methyl ketone; Z-DEVD-fmk, benzyloxycarbonyl-Asp-Glu-Val-Asp-fluoromethyl ketone; dec-RRLL-cmk, decanoyl-Arg-Arg-Leu-Leu-chloromethyl ketone; CREB, cAMP-response element-binding protein; HMG, hydroxymethylglutaryl; HMGCS1, HMG-CoA synthase; CAPS, 3-(cyclohexylamino)propanesulfonic acid; CHAPS, 3-[(3-cholamidopropyl)dimethylammonio]-1-propanesulfonic acid; ATF, activating transcription factor; OASIS, old astrocyte specifically induced substance.

[4] R. J. Midura and J. P. Gorski, manuscript in preparation.

and chemiluminescent digital images were captured with a Fuji LAS-4000.

Anti-SKI-1 antibodies (h-SKI-CT (C terminus specific for amino acids 1036–1051); 723.03 (recognizes pro-SKI-1); 705.02 (recognizes residues 634–651)) (see Pullikotil *et al.* (31, 32) for details) and anti-CREB-H antibodies (33) were gifts from Dr. N. G. Seidah, Institut Recherches Cliniques de Montreal, and Dr. K. Zhang, Wayne State University, respectively. Antibodies against SREBP-1 (amino acids 38–89), SREBP-2 (amino acids 424–473), and GAPDH were purchased from Sigma, and antibodies against OASIS were obtained from Aviva Systems Biology.

Isolation of Nuclear and Cytoplasmic Fractions from UMR106-01 Cultures—UMR106-01 cells were cultured under serum-depleted conditions as described above. Sixty-four hours after plating, the medium was exchanged for mineralization medium (18); some of the cultures were also treated with 100 μM AEBSF, 40 μM dec-RRLL-cmk, or, 10 or 20 μM Z-DEVD-fmk. Cultures were then incubated for an additional 12 h, and the nuclear and cytoplasmic fractions were prepared using a Thermo Scientific NE-PER Nuclear and Cytoplasmic Extraction kit per the manufacturer's instructions. Extracts were separated into aliquots and stored at −80 °C until subjected to Western blotting.

Transfection with Plasmids—UMR106-01 cells were plated in 24-well plates with growth medium containing 10% FBS. At 40 h after plating, transfections were carried out in growth medium containing 1% FBS. Initially, each plasmid was pretitered to determine an optimum dosage; cell cultures were transfected with 0.25–0.75 μg of plasmid DNA at three different levels of Metafectene Pro transfection reagent (Biontex) per the manufacturer's protocol. Individual plasmids and Metafectene Pro reagent were preincubated at room temperature for 20 min before the addition to cells for 24 h, at which time the mixture was exchanged for serum-free mineralization medium containing 0.1% BSA. An optimized dosage of plasmid was used in subsequent studies examining the effect of overexpression of recombinant transcription factors on mineralization. At 88 h after plating, cultures were fixed in 70% ethanol and then stained with 10 μg/ml Alizarin red S dye. Both bright field and fluorescence microscopic images were obtained. Alternatively, calcium was quantitated with a colorimetric assay (16).

Expression plasmids were prepared as follows. cDNAs coding for hSREBP-1a, -1c, and -2 were purchased from Origene. PCR was used to clone their N-terminal fragments and to then tag them with the V5 epitope (GKPIPNPLLGLDST) at their C terminus. The resultant plasmids produced the following proteins: hSREBP1a, amino acids 1–511-V5; SREBP-1c, amino acids 55–511-V5; SREBP-2, amino acids 1–475-V5 (expression plasmids, OASIS TMC, and CREB-H TMC were kindly provided by Dr. P. O'Hare (Marie Curie Research Institute)).

Extraction of Proteins from UMR106-01 Cultures—UMR106-01 cells were seeded in 48-well plates and grown in serum-depleted conditions as described previously (16, 17). During the final 24-h mineralization period, wells were exchanged with mineralization medium containing 0.1% BSA; some of the wells also received 100 μM AEBSF or 40 μM dec-RRLL-cmk. At the conclusion of the culture period, media were removed, inactivated at 95 °C for 5 min, dialyzed against 5% acetic acid, and lyophilized to dryness. The cell layer was extracted as previously described (16); EDTA extracts were immediately inactivated at 95 °C and processed as described above. Subsequent urea/CHAPS cell layer extracts (16) were homogenized and then ultracentrifuged at 30,000 rpm (~100,000 × *g*) for 1 h in an SW50.1 rotor before SDS-PAGE and Western blotting studies.

Laser Microdissection of BMF—UMR106-01 cells were plated onto glass slides, mineralized, and processed for laser micro dissection, extraction, and Western blotting as described by Huffman *et al.* (16).

Primary Calvarial Cell Isolation and Cell Culture—Primary mouse osteoblasts were isolated from calvaria of 5–7-day-old transgenic DMP1 GFP mice (34) using a modification of a published method (35, 36). Briefly, 4 sequential 20-min digests were performed in Hanks' balanced salt solution containing 0.05% trypsin and 0.2% collagenase. Fractions 2–4 were pooled, centrifuged, and re-suspended in minimum essential medium (MEM) α containing 10% FBS, 2 mM L-glutamine, 100 units/ml penicillin, and 30 μg/ml gentamicin (α-growth medium). 2×10^6 cells were plated per T-75-cm^2 flask and allowed to reach confluency. Flasks were then trypsinized and the cells plated onto 48-well culture dishes. At confluency, the media was changed to α-minimum Eagle's medium containing 5% FBS, 50 μg/ml ascorbic acid, 5 mM β-glycerol phosphate, and antibiotics. BGP was omitted from wells that served as un-mineralized controls.

Some cultures were treated on days 6 and 9 with 8 μM dec-RRLL-cmk or 10 μM AEBSF. On day 12, cultures were either incubated with MTT or were fixed with 2% or 4% *p*-formaldehyde and processed for Alizarin red S staining. Images were taken with a Nikon T2000 fluorescence microscope equipped with a CCD camera.

DNA Array—Triplicate UMR106-01 cultures were plated (13, 16) and grown with or without 400 μM AEBSF for 12 h before isolation of total RNA (~5 μg) and then converted to single-stranded cDNA using Superscript II reverse transcriptase (Invitrogen) and the Gene Chip T7 promoter primer kit (note: the minimum effective dose of AEBSF capable of completely blocking mineralization in UMR106-01 cultures is 100 μM in serum-free media and 400 μM in media containing 10% FBS (16)). Single-stranded cDNA was then converted to double-stranded cDNA using DNA polymerase I, DNA ligase and RNase H from *Escherichia coli*. The double-stranded cDNA was purified using a cleanup kit from Affymetrix and converted to biotinylated cRNA by *in vitro* transcription using T7 polymerase and biotinylated ribonucleotides (Affymetrix). This was subsequently fragmented by metal-induced hydrolysis to yield 35–200 base fragments that were hybridized to the Affymetrix Rat Genome 230 Plus 2.0 oligonucleotide arrays. After hybridization, the chip was washed and stained with streptavidin-phycoerythrin before being scanned. An antibody amplification staining protocol that used biotinylated goat IgG followed by a second streptavidin-phycoerythrin staining increased the sensitivity of the assay. The chip was

then scanned, and images were analyzed qualitatively using Affymetrix Gene Chip Operating System Software.

Microarray Data Analysis—CEL data files were imported into Gene Spring GX software (Version 10), and the data were normalized using either the MAS5 or the GCRMA algorithm. The gene list was filtered to exclude those that showed low signal values across all samples (*i.e.* bottom 20th percentile). Selection of statistically significant genes from each expression profile was done using an unpaired *t* test with a *p* value cutoff of <0.05. The multiple testing correction (Benjamini and Hochberg false discovery rate, *p* value <0.05) was integrated within each test. Differential expression was defined as $\geq$1.5-fold change in expression found using both MAS5 and GCRMA analysis. Using this stringent criteria avoids false positives associated with use of MAS5 alone as well as facilitates the ability of GCRMA to account for nonspecific hybridization-related background signal.

Isolation of RNA from Serum-depleted Osteoblastic Cultures and Conversion to cDNA—UMR106-01 cells were plated and grown under serum-depleted conditions (13, 16). At 64 h after plating, the media were exchanged with serum-free mineralization media. At 76 h after plating, media were removed from each well, and cells were quickly lysed with STAT-60 (Tel-Test, Inc.); the lysates were then immediately frozen and stored in liquid nitrogen vapor. Total RNA was isolated according to manufacturer's instructions (Tel-Test, Inc.). Each RNA pellet was washed 2 times with 80% ethanol and then air-dried before resuspending in 10 μl of RNase-free water containing 4% RNasin inhibitor (Promega, Inc.). cDNA was produced using the High Capacity cDNA reverse transcription kit (Applied Biosystems) and stored frozen in aliquots.

For real time PCR, cDNA preparations were diluted and added to 96-well plates containing Taqman Master Mix solution and either the appropriate 6-carboxyfluorescein-labeled expression gene primer set or the VIC-labeled β-actin control primer set (ABI, Inc.). Plates were run on an ABI 7000 Real Time system using pre-programmed software. All calculations were made by the $\Delta\Delta^{CT}$ method by comparison to the β-actin control.

Assay of Caspase-3—Recombinant caspase-3 (Sigma) and lysates of UMR106-01 cultures were assayed using a fluorescent substrate and reagents from Ana-Spec, Inc. (#71118) according to the manufacturer's protocol.

Assay of SKI-1 Peptidase Activity—UMR106-01 cultures were cultured as usual in 48-well plates and treated with inhibitors as described above. The media were exchanged for serum-free medium, the total cell layer was disrupted by scraping into reaction buffer, and aliquots were immediately assayed using a succinylated Tyr-Ile-Ser-Arg-Arg-Leu-Leu-(7-methoxycoumarin-4-acetic acid) (TISRRLL-MCA) substrate (37) and a fluorescent plate reader at 0, 0.5, 1, and 2 h. Rates were extrapolated from kinetic reaction curves.

RESULTS

Activated 105-kDa Form of SKI-1 Is Present in Biomineralization Foci—SKI-1 protease is synthesized as a membrane-bound precursor of 145 kDa (38) and is activated by autolytic cleavage to generate catalytically active 105-kDa (membrane bound) and 98-kDa (shed) forms (38, 39). SKI-1 can be inactivated by the irreversible covalent serine protease inhibitor AEBSF. Because we showed previously that AEBSF blocked mineralization and inhibited fragmentation of BMF biomarkers bone sialoprotein and BAG-75 (16), we asked if active SKI-1 is associated with extracellular biomineralization foci and whether AEBSF alters the distribution of SKI-1 within mineralizing cultures.

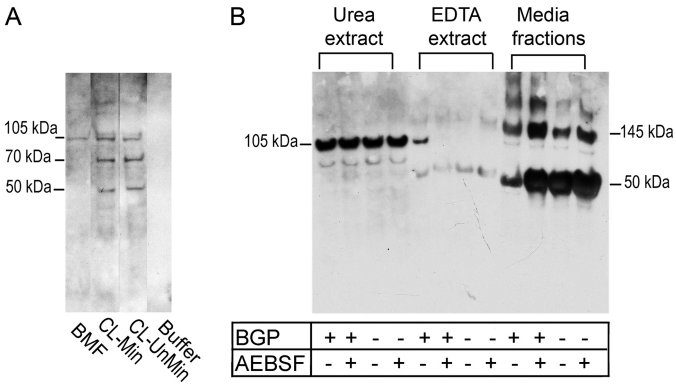

FIGURE 1. **Activated 105-kDa SKI-1 is localized to extracellular calcified biomineralization foci in osteoblastic cultures.** *A*, comparative Western blotting is shown of laser microdissected biomineralization foci with total cell layer extracts from osteoblastic cultures with anti-C-terminal SKI-1 antibodies. UMR106-01 osteoblastic cells were grown on glass slides and allowed to mineralize as described (13), and the resultant mineralized biomineralization foci were isolated by laser microdissection after staining with Alizarin red S dye. Isolated BMF and total cell layer fractions were then extracted and subjected to Western blotting as described previously (16). Six micrograms of protein were applied to each lane. No immunoreactive bands were detected in extraction buffer alone controls (*Buffer*, Fig. 1*A*). *Numbers in the left margin* refer to estimated molecular masses of immunoreactive bands. *BMF*, biomineralization foci isolated by laser micro dissection; *CL-Min*, total cell layer from mineralized culture; *CL-UnMin*, total cell layer from non-mineralized culture; *Buffer*, control for extraction buffer. *B*, shown is comparative Western blotting of cell layer extracts and media fractions from mineralized, AEBSF-inhibited, and non-mineralized osteoblastic cultures. Media were removed, and the residual cell layer fraction was then extracted sequentially with 0.05 M EDTA and with 8 M urea, 0.5% CHAPS as described by Huffman *et al.* (16). Equivalent amounts of each fraction (urea/CHAPS extract, EDTA extract, and media) were subjected to Western blotting with anti-C-terminal SKI-1 antibodies using chemiluminescent detection. *Numbers in the left margin* refer to estimated molecular masses of immunoreactive bands. BGP, with 6.5 mM β-glycerol phosphate; AEBSF, with 100 μM AEBSF.

Mineralized BMF were isolated by laser microdissection from UMR106-01 cultures and Western-blotted with a polyclonal antibody recognizing the C-terminal cytosolic tail of SKI-1 (32). Only the 105-kDa form was present in BMF isolated from mineralized cultures (*lane BMF*, Fig. 1*A*). In contrast, the *CL-Min* and *CL-UnMin lanes* contained the 105-kDa band along with presumed fragments at 70 and 50 kDa (Fig. 1*A*). However, the 70- and 50-kDa components were not detected in microdissected BMF. Whereas the BMF fraction contains only mineralized foci (Fig. 1) (16), *CL-Min* and *CL-UnMin* fractions represent extracts of the cell layer from mineralized and un-mineralized cultures, respectively, which includes cells and BMF.

Cell layers were extracted with a two-step protocol devised to efficiently extract proteins from cells and the extracellular matrix. Mild EDTA extraction predominantly removes materials associated with extracellular BMF complexes, whereas extraction with 8 M urea/CHAPS recovers residual intracellu-

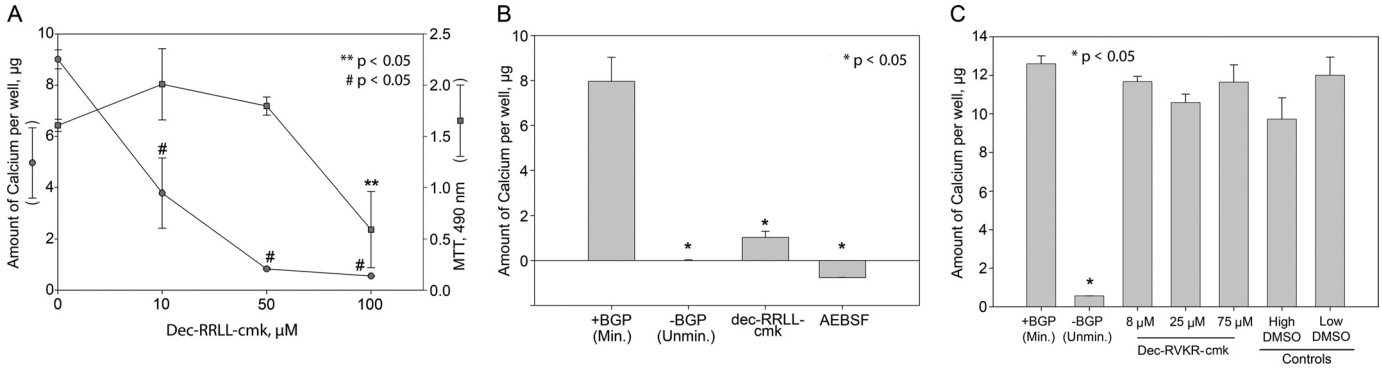

FIGURE 2. **SKI-1-specific inhibitor, dec-RRLL-cmk, like AEBSF, specifically inhibits mineralization in UMR106-01 osteoblastic cultures.** *Error bars* refer to S.D.; probabilities were determined by a one-way analysis of variance with a Student-Newman-Keuls multiple comparison test. *A*, titration of dec-RRLL-cmk demonstrates its capacity to completely block mineralization without affecting cell viability. Osteoblastic cells were grown as usual and treated for 24 h under mineralizing conditions (see under "Experimental Procedures") with different concentrations of inhibitor. Mineralization was assayed with a colorimetric calcium assay by reference to a standard curve; cell viability was determined using the MTT assay. *B*, side-by-side comparison reveals dec-RRLL-cmk and AEBSF both completely block mineralization in culture. *+BGP*, plus β-glycerol phosphate; *−BGP*, minus β-glycerol phosphate; *dec-RRLL-cmk*, 40 μg/ml inhibitor; AEBSF, 100 μM inhibitor. *C*, furin peptide inhibitor dec-RVKR-cmk is without effect on mineralization. *+BGP*, plus β-glycerol phosphate; *−BGP*, minus β-glycerol phosphate; *dec-RVKR-cmk*, range of concentrations from 8 to 75 μmol; *DMSO*, high and low represent solvent controls.

TABLE 1

The effect of inhibitors on total cellular SKI-1 peptidase activity

Replicate cultures ($n = 6$) were stopped 8 h after the addition of BGP and SKI-1 assays, carried out on total cell lysates as described under "Experimental Procedures." Data were analyzed using one-way analysis of variance with a Student-Newman-Keuls multiple comparison test. Data are representative of duplicate experiments.

Culture condition	Peptidase activity ±S.D.	Percent of control	Statistical significance
	(Arbitrary fluorescence units/h/culture well) × 1000	*%*	
Mineralizing control (+BGP)	1616 ± 58.3	100 ± 3.6	
+100 μM AEBSF +BGP	1161 ± 145.0	71.8 ± 12.5	$p < 0.05$
+50 μM dec-RRLL-cmk +BGP	986 ± 125.6	61.0 ± 12.7	$p < 0.05$
+20 μM DEVD-OPH +BGP	1727 ± 67.9	106.8 ± 3.9	
+75 μM dec-RVKR-cmk +BGP	1807 ± 119.0	111.8 ± 6.6	

lar and extracellular matrix components (16). Activated 105-kDa SKI-1 was present in the EDTA extract but absent from AEBSF-treated or un-mineralized cultures (Fig. 1*B*), suggesting that transport of SKI-1 to extracellular BMF occurs only during mineralization. Urea/CHAPS extracts contained similar amounts of 105-kDa SKI-1 regardless of the culture condition. The culture media contained 145-kDa SKI-1 precursor and a 50-kDa fragment band. Due to the specificity of the antibody and the structure of SKI-1 (31, 32, 38, 39), we assume that all forms detected (145, 105, 70, and 50 kDa) contain the transmembrane sequence and are associated with membranes or vesicles released from cells. Interestingly, the amount of 50-kDa band in the media was found to be lower in mineralized cultures, indicating that breakdown of SKI-1 may be increased under non-mineralizing conditions (Fig. 1*B*).

Treatment of Osteoblastic Cultures with a Specific SKI-1 Inhibitor Also Blocks Mineralization—The structure of dec-RRLL-cmk is based on the preferred substrate specificity of SKI-1 and is more specific than AEBSF (32, 37, 38). When UMR106-01 cells were treated with dec-RRLL-cmk, mineralization was progressively blocked, as the concentration of inhibitor was increased (Fig. 2*A*). Forty micromolar dec-RRLL-cmk represents a minimum effective inhibitory dose compared with 100 μM AEBSF (Fig. 2, *A* and *B*) (16). By contrast, a structurally similar furin inhibitor (40), dec-RVKR-cmk, was without effect (Fig. 2*C*) Importantly, assays of treated cultures also demonstrated that AEBSF and dec-RRLL-cmk significantly decreased SKI-1 peptidase activity by about 30 and 40%, respectively, whereas treatment with other inhibitors containing analogous reactive functional groups were without a negative effect (Table 1). AEBSF and dec-RRLL-cmk do not significantly decrease cell number (Fig. 1) (16), whereas Z-DEVD-OPH and dec-RVKR-cmk reduce cell viability by no more than 15% (not shown).

We also treated primary calvarial osteoblastic cultures from transgenic DMP1-GFP mice (34–36) with dec-RRLL-cmk. Because GFP expression precedes mineralization in these cultures, this protein serves as a marker of where and when mineralization will occur in these longer term cultures. Osteoblastic precursors were plated onto collagen-coated wells and grown under mineralizing conditions for up to 12 days in the presence of either 0, 1, or 8 μM dec-RRLL-cmk. Concentrations of AEBSF and dec-RRLL-cmk were lowered to accommodate the longer exposure with primary cells *versus* UMR106-01 cells. Mineral crystals were detected by staining with Alizarin red S and correlated with GFP expression. Focal areas of GFP-positive cells generally appeared about 6–8 days after plating and went on to form mineralized nodules by about day 12 (Fig. 3*A*). Exposure to 8 μM dec-RRLL-cmk inhibitor diminished expression of the DMP1-GFP reporter (Fig. 3*B*) as well as blocking mineralization. As a positive control, 10 μM AEBSF also completely blocked mineralization and DMP1-GFP reporter expression by primary calvarial cultures (16) (Fig. 3*C*). These results indicate that SKI-1 is required for progression through the osteoblastic mineralization stage and the transition to the embedded osteoblast or osteocyte stage.

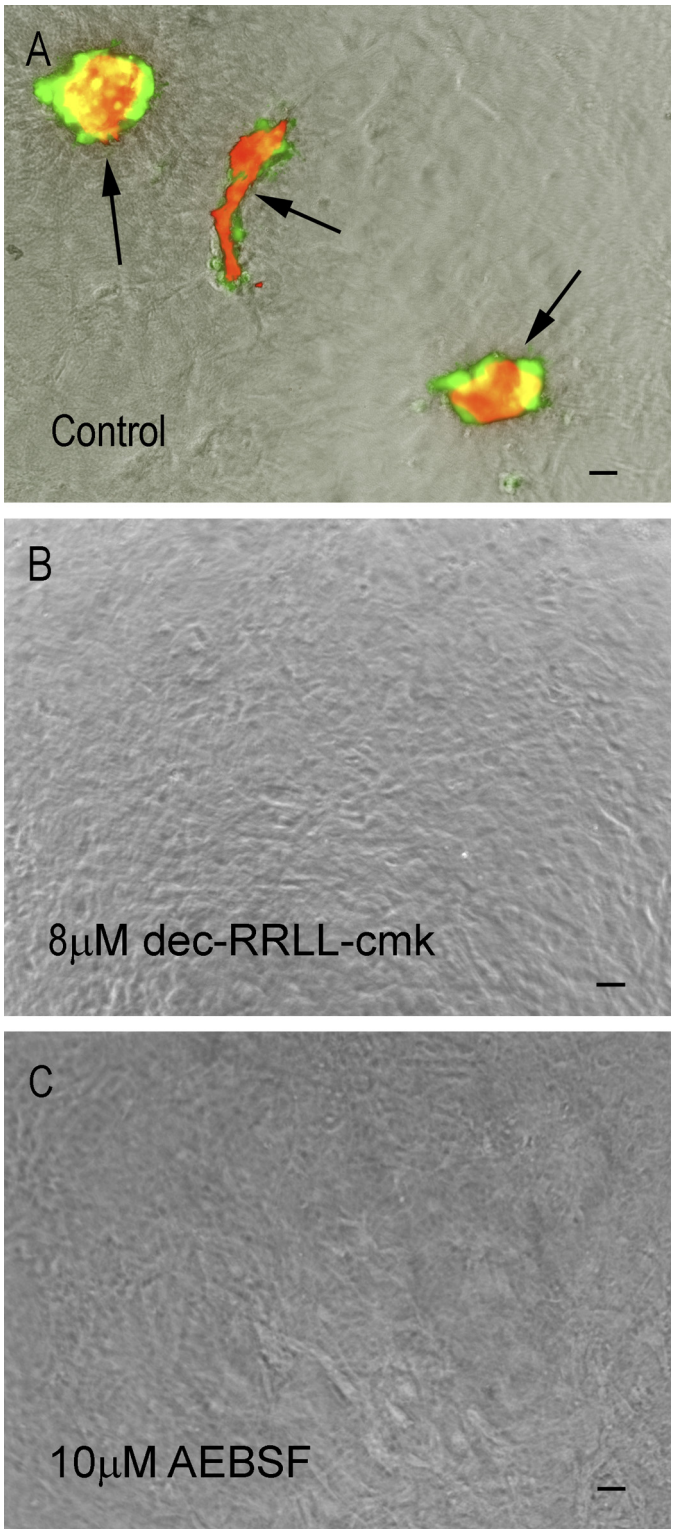

FIGURE 3. **SKI-1 inhibitor dec-RRLL-cmk also blocks mineralization of primary mouse calvarial osteoblastic cells.** Primary mouse calvarial cells from transgenic DMP1 GFP mice (34) were harvested by a conventional sequential collagenase digestion protocol and plated as noted under "Experimental Procedures." The media was changed at 3-day intervals starting on day 3 after plating. Some cultures were treated with SKI-1 inhibitors. *Scale bars* = 375 μm. *A*, control calvarial cells produced mineralized nodules on day 12 after plating. Mineralized nodules were detected by fluorescence microscopy after staining the culture with 10 μg/ml Alizarin red S dye. The green fluorescent signal represents GFP protein expressed under control of the 10-kb Dmp1 promoter. *Yellow* represents areas of overlap of mineral (*red*) and GFP (*green*) signals. *Arrows* demark mineralized areas, which also express GFP protein. *B*, dec-RRLL-cmk blocks the mineralization of primary calvarial cells as well as expression of GFP protein. Cells were treated continuously from day 3 until day 12 with 8 μM dec-RRLL-cmk inhibitor, and then the cultures were imaged by fluorescence microscopy as in *A*. *C*, AEBSF inhibits the mineralization of primary calvarial cells as well as expression of GFP protein. Cells were treated continuously from day 3 until day 12 with 10 μM AEBSF inhibitor, and then the cultures were imaged by fluorescence microscopy as in *A*.

Short Term Treatment of Osteoblastic Cells with AEBSF Decreases Transcription of Mineralization-related Genes—Because SKI-1 and site-2 catalyze the release of activated transcription factors from the cis/medial Golgi (19), we asked whether AEBSF blocks transcription of mineralization-related genes. UMR106-01 cultures were treated for 12 h (from 64–76 h after plating) with or without a minimum concentration of AEBSF sufficient to block mineralization. UMR106-01 cultures begin to nucleate calcium phosphate crystals within biomineralization foci at 76 h (16, 17). Total RNA was isolated, converted to cDNA before labeling, and incubated with whole rat genome arrays (see "Experimental Procedures" for details).

AEBSF treatment reduced expression of 140 genes by 1.5–3-fold, whereas 38 genes were found to be increased by at least 1.5-fold (array data has been deposited with the Gene Expression Omnibus data base (series accession number GSE21476)). It is noteworthy that genes encoding a number of mineralization related extracellular matrix proteins were reduced (Table 2), *e.g.* DMP1, type I procollagen α1 and α2 chains, type XI procollagen α1 chain, fibronectin, matrilin 3, ectonucleotide pyrophosphatase/phosphodiesterase 2 and 3, and tenascin-C and -N. Interestingly, the reduced expression for *DMP1* observed (Table 2) is consistent with the lack of DMP1-GFP transgene expression noted in primary calvarial cultures treated with these inhibitors (Fig. 3).

dec-RRLL-cmk Also Blocks Transcription of Dmp1, Phex, FN1, COL11A1 Genes—Because dec-RRLL-cmk is a more specific inhibitor of SKI-1 than AEBSF (20), we predicted that it should reproduce those actions of AEBSF (Table 2), which are mediated by SKI-1. To test this, UMR106-01 cultures were again treated for 12 h with 40 μM dec-RRLL-cmk (Fig. 2). Parallel cultures were also treated with AEBSF (16) (Fig. 2*B*). This study was carried out under conditions of serum deprivation to reduce exposure to cholesterol, which inhibits SCAP (SREBF cleavage-activating protein)-mediated transport of SREBPs toward the cis/medial Golgi where they are activated by SKI-1 and site-2 (41). We showed earlier that the amount of mineral deposited in UMR106-01 cultures is unaffected by serum depletion (16).

Total RNA was isolated and converted to cDNA. Quantitative PCR was then carried out on a representative group of genes decreased by AEBSF (Table 2). Expression of HMG-CoA synthase (HMGCS1) was also included as a positive control as it is regulated by SREBP transcription factors activated by SKI-1 (42, 43). Other cultures were treated with inhibitors until 88 h when the amount of mineralization was determined. As expected, both inhibitors blocked mineralization by greater than 90% (data not shown but similar to that in Fig. 2*B*).

TABLE 2
AEBSF blocks transcription of a number of key mineralization-related genes in a whole array study with UMR106–01 cells

-Fold change	Gene symbol	Description
−1.58	*Hsd17b11*	Hydroxysteroid (17-β) dehydrogenase 11
−1.59	*Senp7*	SUMO1/sentrin-specific protease 7
−1.64	*Adamtsl1*	AdamTS1-like protease
−1.66	*Phex*	Phosphate-regulating gene with homologies to endopeptidases on the X chromosome
−1.67	*Casp4*	Caspase 4
−1.77	*Enpp3*	Alkaline phosphodiesterase
−1.85	*Fbn2*	Fibrillin 2
−1.90	*Enpp2*	Ectonucleotide pyrophosphatase/phosphodiesterase 2
−1.90	*Tnc*	Tenascin C
−1.91	*pColA1 (I)*	Procollagen, type I, α1 chain
−1.94	*Mitf*	Microphthalmia-associated transcription factor
−1.97	*Atp1a2*	ATPase, Na^+K^+ transporting, α2
−1.97	*Tnn*	Tenascin N
−1.98	*Fn*	Fibronectin 1
−2.10	*Scn1a*	Sodium channel voltage-gated, type 1α
−2.13	*pColA1(XI)*	Procollagen, type XI, α1 chain
−2.18	*pColA2(I)*	Procollagen, type I, α2 chain
−2.28	*Acss2*	Acyl-CoA synthetase short chain family member 2
−2.37	*Serpini1*	Serine (cysteine) peptidase inhibitor
−2.50	*DMP-1*	Dentin matrix protein-1
−2.55	*pColA2(I)*	Procollagen, type I, α2 chain
−2.99	*Matn3*	Matrilin 3

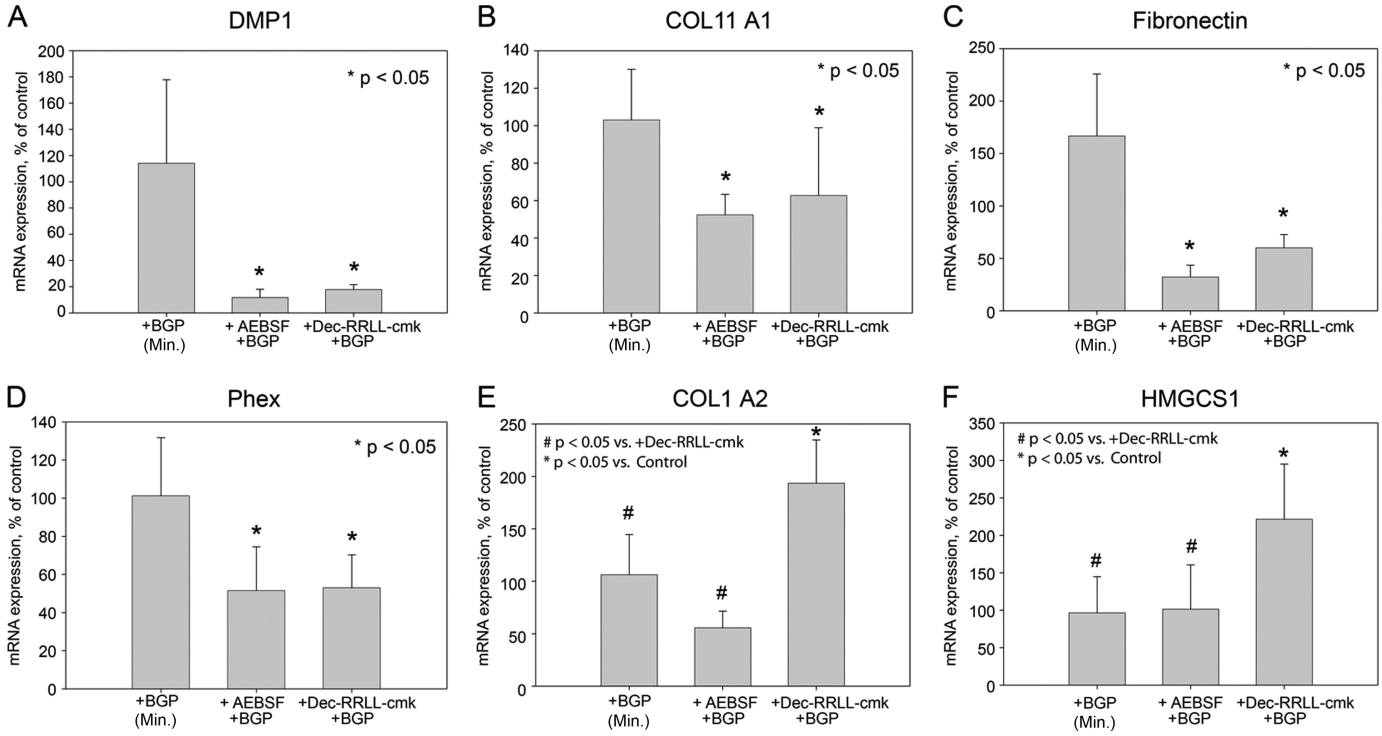

FIGURE 4. **dec-RRLL-cmk and AEBSF block expression by UMR106-01 osteoblastic cells of key genes required for mineralization and for normal bone formation.** Total RNA was isolated from replicate cultures ($n = 6$/condition) treated for 12 h with β-glycerol phosphate with or without inhibitors and converted into cDNA with reverse transcriptase (see "Experimental Procedures"). Quantitative PCR was carried out using primer sets for individual genes, and the relative expression for each gene was plotted as a percentage of that expressed by mineralized control cultures. *Error bars* refer to S.D., and probabilities were calculated using a one-way analysis of variance test. *+BGP*, control cultures treated with mineralizing conditions (6.5 mM β-glycerol phosphate); *+AEBSF+BGP*, cultures treated for 12 h with 100 μM AEBSF under mineralizing conditions; *+dec-RRLL-cmk+BGP*, cultures treated for 12 h with 40 μM dec-RRLL-cmk under mineralizing conditions. *A–F*, shown are quantitative PCR results for *Dmp1*, *COL11A1*, fibronectin, *Phex*, *COL1A2*, and *HMGCS1* genes.

All quantitative PCR results are plotted in Fig. 4 as a percentage of the expression in cultures treated with mineralizing conditions. Visual inspection of the data reveals two patterns. First, expression of *DMP1*, procollagen XI α1 chain, *Phex*, and fibronectin was significantly decreased by each SKI-1 inhibitor (Figs. 4, *A–D*). For each gene, the average knockdown with AEBSF was found to be quantitatively greater than that for dec-RRLL-cmk (Figs. 4, *A–D*), but differences were not significant. In the second pattern, highest expression of *COL1 A2* and *HMGCS1* occurred in dec-RRLL-cmk-treated cultures, whereas that for mineralizing control or for AEBSF-treated culture was found to be significantly lower (Fig. 4, *E* and *F*). Expression of *HMGCS1* in AEBSF-treated cells was indistinguishable from controls (*+BGP*, Fig. 4*E*), whereas expression of *COL1 A2* was lower in AEBSF-treated cells than controls (*+BGP versus AEBSF+BGP*, $p = 0.05$, Fig. 4*E*). The quantitative PCR results with AEBSF are very similar to array results for *DMP1*, procollagen XI α1 chain, *Phex*, fi-

bronectin, and *COL1 A2* (Table 2). The results for *HMGCS1* were unexpected as its expression is tightly regulated by SREBP-1 and SREBP-2 (42, 43) and, thus, should be dependent upon SKI-1. Based on quantitative PCR results, mineralization in UMR106-01 cultures correlates most closely with the expression of *DMP1*, *COL11 A1*, fibronectin, and *Phex* (compare Figs. 2 and 4).

Activation of Caspase-3 Is Regulated Differently in AEBSF and dec-RRLL-cmk-treated Cultures—As first shown by Wang *et al.* (20, 21), activation of SREBP-1 and SREBP-2 can be also mediated by caspase-3. Caspase-3 and SKI-1 cleave these factors at different sites producing different sized, transcriptionally active N-terminal fragments (21, 22). We, therefore, tested whether a caspase-3/-7 specific inhibitor would also inhibit mineralization of BMF. Interestingly, 10 and 20 μM Z-DEVD-fmk had no significant effect on mineralization in UMR106-01 cultures (Fig. 5*A*). By comparison, 100 μM AEBSF and 50 μM dec-RRLL-cmk blocked mineralization by >85% (Fig. 5*A*).

To determine whether caspase-3 was specifically inactivated by Z-DEVD-fmk, the cytosolic fraction of cell lysates was assayed using a small fluorescent peptide substrate. Caspase-7 is predominantly membrane-bound (44) under these conditions and should have been removed by centrifugation before assays. Intracellular caspase-3 catalytic activity was blocked by up to 80% by Z-DEVD-fmk and was also reduced about 60% by dec-RRLL-cmk (Fig. 5*B*). However, AEBSF had no effect. To establish if dec-RRLL-cmk directly inactivated caspase-3, we incubated recombinant caspase-3 with various inhibitors for 30 min and then measured its catalytic function. As shown in Fig. 5*C*, 50 μM dec-RRLL-cmk and 100 μM AEBSF were all without effect, suggesting that the former acts indirectly to block procaspase-3 activation.

In view of the differential gene expression patterns observed with AEBSF- and dec-RRLL-cmk-treated osteoblastic cultures (Fig. 4), we next asked whether the amount of activated caspase-3 protein varied as a function of the inhibitor used. UMR106-01 cultures were treated for 12 h with a series of inhibitors as described in Fig. 5. Cell layers were then dissociated in hot SDS-8M urea solution containing an excess of DTT, and fractions were processed for Western blotting. The total cellular content of activated 19-kDa caspase-3 (45) was similar in mineralized, un-mineralized, and AEBSF-treated cultures (Fig. 5*D*). However, the caspase-3 content of dec-RRLL-cmk-treated cultures was greatly reduced (*arrow*, Fig. 5*D*). By comparison, blots processed for control protein GAPDH gave similar band intensities for all conditions (Fig. 5*E*). These results also suggest that activation of procaspase-3 is decreased in dec-RRLL-cmk-treated cultures compared with mineralized, un-mineralized, and AEBSF-treated cultures. Finally, the content of 19-kDa caspase-3 was noticeably higher in cultures treated with 10 and 20 μM Z-DEVD-fmk or Z-DEVD-OPH than in controls (*arrowheads*, Fig. 5*D*).

Treatment of UMR106-01 Cells with AEBSF or with dec-RRLL-cmk Alters the Nuclear Content of SKI-1-activated Transcription Factors—To further test if SKI-1 is required for activation of SREBP and CREB/ATF family transcription factors, which are imported into the nucleus where they control the expression of mineralization related genes, we asked whether AEBSF or dec-RRLL-cmk reduced the nuclear content of selected transcription factors. Commonly, cells grown in 10% fetal bovine serum have been used as a control for caspase-3 activation as the serum cholesterol leads to feedback inhibition of SKI-1 activation of SREBPs. As a result, Western blotting was used to identify the activating protease from the nuclear sizes of activated transcription factors.

To select which transcription factors to investigate, we searched for conserved transcription factor binding sites in the proximal promoter regions of the *PHEX*, *DMP1*, *FN1*, *COL11A1*, *COL1A2*, and *HMGCS1* genes using the NCBI ECR Browser program. This analysis revealed that consensus SRE and CRE sequences exist in all of the six 5′-proximal promoter regions (not shown). Additionally, OASIS was shown recently to be required for normal bone formation (25, 26), and CREB-H (CREB3L3) represents a CREB/ATF family member activated by SKI-1 (33). Expression of HMGCS1 is also regulated primarily by SREBP-1 and SREBP-2 (42, 43). Based on these findings, we focused our analyses on a mix of SRE and cyclic AMP response element (CRE) binding factors: SREBP-1, CREB-H (CREB3L3), OASIS (CREB3L1), and SREBP-2.

UMR106-01 cells were plated as usual in 10% fetal bovine serum (16), and at 64 h, the media were exchanged again for serum-free media containing either BGP alone (mineralizing conditions) or with AEBSF, dec-RRLL-cmk, or Z-DEVD-fmk. Because AEBSF and dec-RRLL-cmk required only 12 h to reduce transcription of key mineralization genes (see Fig. 4), we also stopped these cultures 12 h after the addition of inhibitors. Nuclear (Fig. 6) and cytoplasmic (Fig. 7) fractions were then immediately prepared for Western blotting.

Nuclear OASIS consisted of a 58-kDa SKI-1-activated form (*OASIS panel*, Fig. 6). This assignment is consistent with the findings of Omori *et al.* (46). The nuclear content of 58-kDa OASIS was lower in both the AEBSF- and dec-RRLL-cmk-treated cultures (*OASIS panel*, Fig. 6). Parallel controls with cytoplasmic extracts from these same cultures were blotted against GADPH and show that the observed changes were not due to differences in sample loading (see Fig. 7). These results indicate that AEBSF and dec-RRLL-cmk both reduce the nuclear content of SKI-1-activated 58-kDa OASIS.

In contrast to OASIS, the nuclear content of CREB-H did not change when AEBSF or dec-RRLL-cmk was included. Consistent with other work with this antibody (32), a 42-kDa band (SKI-1-activated) and doublet immunoreactive bands containing 42 (SKI-1-activated)- and 45-kDa (caspase-3-activated) forms were detected in +FBS cultures (*CREB-H panel*, Fig. 6). Thus, CREB-H does not play a role in transcriptional changes brought about by AEBSF or dec-RRLL-cmk (Fig. 4).

The nuclear content of 68-kDa activated SREBP-2 was reproducibly decreased by both AEBSF and dec-RRLL-cmk (*SREBP-2 panel*, Fig. 6). By comparison, nuclei from +FBS-treated cultures contained two closely spaced activated SREBP-2 forms at 68 kDa (SKI-1 cleavage) and at 65 kDa (presumed to be cleaved by caspase-3). The nuclear content of 68-kDa SREBP-2 is reduced in cultures treated for 12 h with either AEBSF or dec-RRLL-cmk.

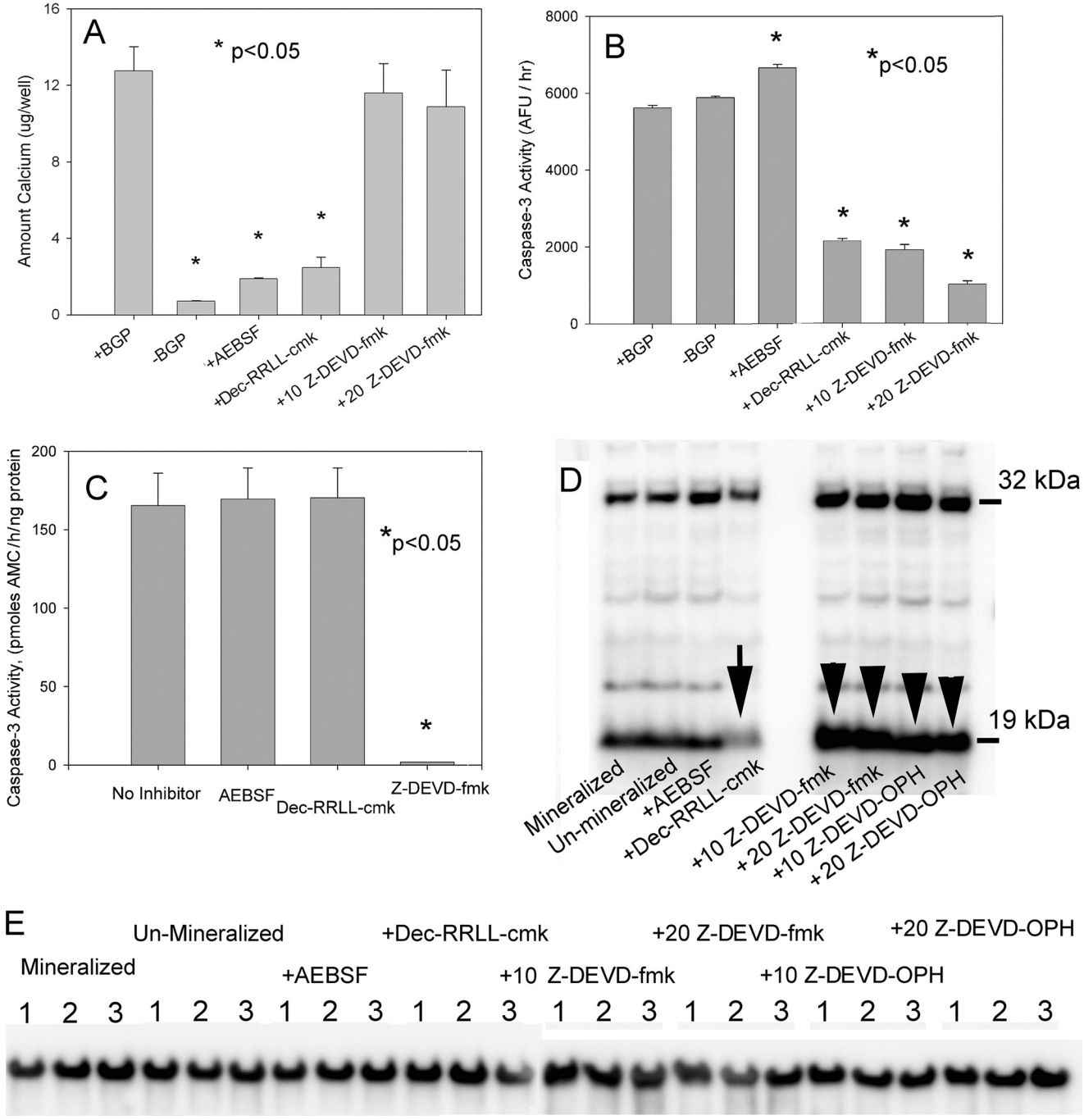

FIGURE 5. **dec-RRLL-fmk partially blocks activation of caspase-3, although caspase-3 inhibitors do not inhibit osteoblast-mediated mineralization.** UMR106-01 cultures were treated with β-glycerol phosphate with or without inhibitors, and then cell layer fractions were assayed for soluble caspase-3 activity, mineral calcium content, and caspase-3 protein content by Western blotting as described under "Experimental Procedures." The direct effects of inhibitors on recombinant caspase-3 were analyzed separately. *Error bars* represent S.D., and probabilities were tested with a one-way analysis of variance test using a Student-Newman-Keuls multiple comparison test. *Mineralized*, cells treated with β-glycerol phosphate; *Un-mineralized*, no β-glycerol phosphate; *+AEBSF*, cells treated with 100 μM inhibitor and β-glycerol phosphate; *+dec-RRLL-cmk*, cells treated with 40–50 μM inhibitor and β-glycerol phosphate; *+10 Z-DEVD-fmk*, cells treated with 10 μM inhibitor and β-glycerol phosphate; *+20 Z-DEVD-fmk*, cells treated with 20 μM inhibitor and β-glycerol phosphate; *+10 Z-DEVD-OPH*, cells treated with 10 μM inhibitor and β-glycerol phosphate; *+20 Z-DEVD-OPH*, cells treated with 20 μM inhibitor and β-glycerol phosphate. All results are representative of at least duplicate experiments. *A*, treatment of UMR106-01 osteoblastic cultures with Z-DEVD-fmk does not block mineralization. The average amount of calcium deposited in biomineralization foci was then determined colorimetrically ($n = 6$). *B*, Z-DEVD-fmk and dec-RRLL-cmk led to significant reductions in intracellular caspase-3 activity. Soluble intracellular caspase-3 activity was extrapolated from kinetic reaction plots; the averaged data is plotted as arbitrary fluorescence units (*AFU*)/h ($n = 6$). *C*, dec-RRLL-cmk does not directly inactivate recombinant caspase-3. Activity was extrapolated from kinetic reaction plots and is plotted as the average nmol of amidomethylcoumarin (*AMC*) released/h/ng of protein ($n = 6$). *D*, shown is a Western blot analysis for precursor and activated caspase-3 forms. The amount of 32-kDa procaspase-3 and intracellular-activated 19-kDa caspase-3 subunit varies depending upon the protease inhibitor treatment. The total cell layer of treated UMR106-01 cultures was extracted with hot SDS/urea sample buffer and subjected to Western blotting with anti-caspase-3 antibodies. The pattern is representative of triplicate experiments. The *arrow* denotes the decreased 19-kDa band in dec-RRLL-cmk treated cells; *arrowheads* demark increased 19-kDa-band content in cells that were treated with caspase-3 Z-DEVD-fmk or Z-DEVD-OPH inhibitor. *E*, shown is a Western blot for intracellular GAPDH control. The cell layers in triplicate wells were extracted with hot SDS/urea sample buffer and subjected to Western blotting with anti-GADPH antibodies.

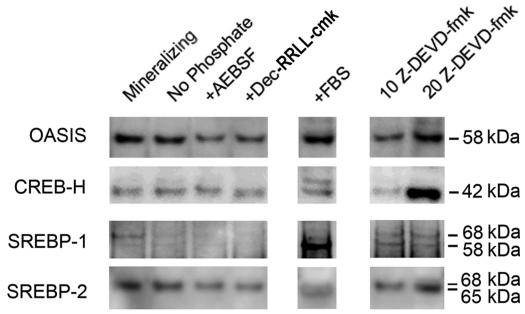

FIGURE 6. **AEBSF, dec-RRLL-cmk, and Z-DEVD-fmk inhibitors alter the nuclear content of SKI-1-activated transcription factor(s).** Cultures were treated for 12 h under mineralizing conditions with different protease inhibitors, and the nuclear fraction was then isolated. All culture conditions were carried out in triplicate, and Western blotting results for OASIS, CREB-H, SREBP-1, and SREBP-2 depicted are representative of these replicates. Cytoplasmic fractions were also isolated from these same cultures, and Western blots for control protein GAPDH are shown in Fig. 7. All lanes shown for each different transcription factor were imaged similarly and at the same time. *Mineralizing*, cells treated with mineralizing conditions (6.5 mM β-glycerol phosphate); *No Phosphate*, no β-glycerol phosphate added; *+AEBSF*, cells treated with 100 μM inhibitor; *+dec-RRLL-cmk*, cells treated with 40 μM dec-RRLL-cmk; *10 Z-DEVD-fmk*, cells treated with 10 μM inhibitor; *20 Z-DEVD-fmk*, cells treated with 20 μM inhibitor. *OASIS panel*, nuclear fractions subjected to Western blotting for OASIS are shown. *CREB-H panel*, nuclear fractions subjected to Western blotting for CREB-H are shown. *SREBP-1 panel*, nuclear fractions subjected to Western blotting for SREBP-1 are shown. *SREBP-2 panel*, nuclear fractions subjected to Western blotting for SREBP-2 are shown.

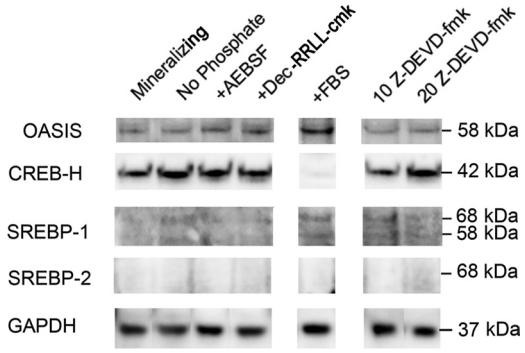

FIGURE 7. **Cytoplasmic contents of selected SKI-1-activated transcription factors.** Cultures were treated for 12 h under mineralizing conditions with different protease inhibitors, and then the cytoplasmic fraction was isolated from each using a commercial kit. All culture conditions were carried out in triplicate, results shown are representative of these replicates, and GAPDH Western blots were used to control for intraculture variations. Nuclear fractions were also isolated from these same cultures. All lanes shown on each panel below were imaged similarly and at the same time. *Mineralizing*, cells treated with 6.5 mM β-glycerol phosphate; *No Phosphate*, no β-glycerol phosphate added; *+AEBSF*, cells treated with 100 μM inhibitor; *+dec-RRLL-cmk*, cells treated with 40 μM dec-RRLL-cmk; *10 Z-DEVD-fmk*, cells treated with 10 μM inhibitor; *20 Z-DEVD-fmk*, cells treated with 20 μM inhibitor. *OASIS panel*, cytoplasmic fractions subjected to Western blotting for OASIS are shown. *CREB-H panel*, cytoplasmic fractions subjected to Western blotting for CREB-H are shown. *SREBP-1 panel*, cytoplasmic fractions subjected to Western blotting for SREBP-1 are shown. *SREBP-2 panel*, cytoplasmic fractions subjected to Western blotting for SREBP-2 are shown. *GAPDH panel*, cytoplasmic fractions subjected to Western blotting for GAPDH are shown.

SKI-1-activated SREBP-1 is also 68 kDa (20, 21), as shown in the mineralized control (*SREBP-1 panel*, Fig. 6). This band is largely absent in non-mineralizing conditions (*No Phosphate*, *AEBSF*, and *dec-RRLL-cmk*) (*SREBP-1 panel*, Fig. 6). A separate 58-kDa form of SREBP-1 (produced by caspase-3) is present in +FBS cultures (20, 21).

To confirm the assignment of caspase-3 cleaved transcription factors in Fig. 6, we isolated nuclear and cytoplasmic fractions from osteoblastic cultures treated with 10 and 20 μM Z-DEVD-fmk (Figs. 6 and 7). Our results show that the nuclear content of CREB-H was increased in cultures treated with 20 μM as compared with +BGP alone (*CREB-H panel*, Fig. 6). The 42-kDa size of the activated nuclear CREB-H form whose content increased with 20 μM Z-DEVD-fmk is consistent with its cleavage by SKI-1 (*CREB-H panel*, Fig. 6).

The Effect of AEBSF and dec-RRLL-cmk Inhibitors on Cytoplasmic SKI-1-activated Transcription Factors—Cytoplasmic transcription factor analysis provides a useful comparison with the nuclear profiles presented in Fig. 6. Although carried out in triplicate, single representative patterns are presented in Fig. 7. In contrast to the nuclear results, the content of cytoplasmic 58-kDa OASIS did not appear to correlate with the presence or absence of inhibitors (Fig. 7). Cytoplasmic CREB-H consisted only of the SKI-1-activated 42-kDa form (33), and its content also did not vary in the presence of inhibitors (*CREB-H panel*, Fig. 7). In support of this assignment, the 42-kDa form was absent from +FBS cultures.

In contrast to results with nuclear fractions, analyses for cytoplasmic SREBP-2 revealed no detectable band under any culture condition (*SREBP-2 panel*, Fig. 7). Also, Western blotting results for SREBP-1 yielded faint doublet bands at 68 (SKI-1-activated)- and 58-kDa (caspase-3-activated) primarily in the FBS- and Z-DEVD-fmk-treated cultures (*SREBP-1 panel*, Fig. 7). However, the content of cytoplasmic SREBP-1 forms did not change with inhibitors. Finally, the content of control protein GAPDH in cytoplasmic extracts was constant among the different conditions (*GADPH panel*, Fig. 7).

Overexpression of SKI-1-activated SREBP-1 Increases Mineralization in UMR106-01 Cultures—To further test our hypothesis that osteoblastic mineralization is dependent upon SKI-1-catalyzed activation of SREBP and CREB/ATF family transcription factors, we transiently overexpressed SKI-1-activated transcription factors (SREBP-1a, SREBP-1c, SREBP-2, OASIS, and CREB-H) in UMR106-01 cells. Plasmids were used that express active transcription factors retaining their nuclear import sequences and bZIP DNA binding domains but missing their C-terminal membrane insertion sequences. All plasmids were compared over the same transfection dosage range, which was optimized for SREBP-1a in initial titration studies. Results are presented visually in Fig. 8 after fluorescent staining for calcium mineral with Alizarin red S.

Overexpression of SREBP-1a resulted in a significant increase in mineralized BMF complexes compared with the non-plasmid control or with cells transfected with OASIS, SREBP-2, or SREBP-1c (Fig. 8). In a separate experiment, SREBP-1a-transfected cells contained 1.32-fold more calcium in mineral deposits compared with the non-plasmid control ($p < 0.05$). Thus, overexpression of SREBP-1a was able to increase both the number of biomineralization foci and the amount of calcium mineral deposited by UMR106-01 osteoblastic cells. Also, CREB-H-transfected UMR106-01 cells exhibited an unusual morphological appearance. In contrast to their usual dispersed appearance, BMFs in CREB-H-trans-

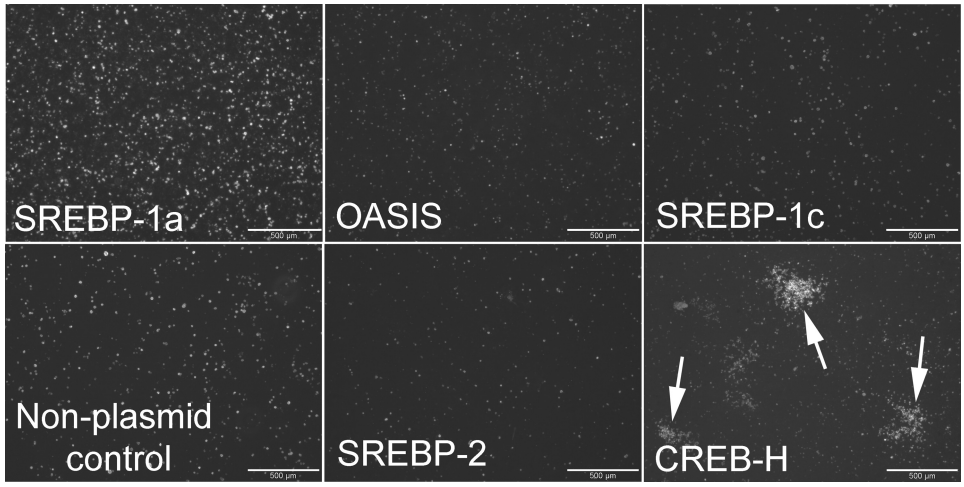

FIGURE 8. **Overexpression of activated forms of SREBP-1a and CREB-H in UMR106-01 cells increases the number and clustering of mineralized biomineralization foci, respectively.** Forty hours after plating, cells were transiently transfected with plasmid in the presence of Metafectamine Pro and grown under standard mineralizing conditions (see "Experimental Procedures"). At 88 h, cultures were fixed with 70% ethanol, stained with Alizarin red S dye, and photographed using a fluorescence microscope. Mineralized BMF appear as *white dots* or *clusters* (*arrows*) under these conditions. Overexpression with activated OASIS, SREBP-1c, and SREBP-2 was without effect and indistinguishable from non-plasmid control cultures. Calcium assays revealed that SREBP-1a-transfected cells deposited 1.32-fold more hydroxyapatite than non-plasmid control cells ($p < 0.05$). *Scale bar* = 500 μm.

fected cells were clumped together in discrete regions that resembled mineralization nodules seen in primary calvarial osteoblastic cultures (see Fig. 3).

DISCUSSION

We show here that mineralization, a property of differentiated osteoblastic cells, is blocked by covalent serine protease inhibitors AEBSF and dec-RRLL-cmk in two osteoblastic culture models. Because both inhibitors inactivate SKI-1, an intracellular cis/medial-Golgi protease required for activation of SREBP and CREB/ATF family transcription factors, we examined the effect of these inhibitors on gene expression. Short term (12 h) treatment of osteoblastic cultures with AEBSF decreased expression of 140 genes by 1.5–3.0-fold including *Phex*, *Dmp1*, *COL1A1*, *COL1A2*, *COL11A1*, and fibronectin. A subsequent comparison of AEBSF with dec-RRLL-cmk, a more specific SKI-1 inhibitor, on expression of a subset of these genes revealed two different outcomes. *Phex*, *Dmp1*, *COL11A1*, and fibronectin were significantly reduced by both inhibitors. *COL1A2* and *HMGCS1*, a positive control for SKI-1 activity (42, 43), were also inhibited by AEBSF, but in contrast, expression was increased by dec-RRLL-cmk relative to mineralizing cultures. AEBSF and dec-RRLL-cmk also reduced the nuclear content of activated forms of OASIS, SREBP-1, and SREBP-2. Because caspase-3 is known to activate SREBP-1 and SREBP-2 (20, 21), we also tested caspase-3/capase-7 inhibitors, but Z-DEVD-fmk did not block osteoblastic mineralization. However, the activation and turnover of caspase-3 was differentially modified depending upon the inhibitor used, *e.g.* AEBSF, dec-RRLL-cmk, or Z-DEVD-fmk. In contrast to AEBSF, the actions of dec-RRLL-cmk represent the sum of its direct actions on SKI-1 and indirect actions on caspase-3. Specifically, dec-RRLL-cmk reduced intracellular caspase-3 activity by blocking the formation of activated 19-kDa caspase-3. Finally, overexpression of the SKI-1-activated forms of SREBP-1a and of CREB-H in UMR106-01 osteoblastic cells increased the number of mineralized foci and altered their local distribution, respectively. These findings suggest that expression of key genes (*Phex*, *Dmp1*, *COL11A1*, and fibronectin) needed for mineralization of osteoblastic cultures *in vitro* and for bone formation *in vivo* are regulated by SREBP and CREB/ATF family transcription factors, which require SKI-1 for their activation.

Intracellular and Extracellular Roles for SKI-1 in Osteoblastic Mineralization—Mineralization in UMR106-01 cultures is a temporally synchronized process, and the first mineral crystals begin to form 12 h after the addition of exogenous phosphate (13, 16, 17). If phosphate is not added or if AEBSF is included, mineralization does not occur (16, 17). AEBSF also blocks the fragmentation of phosphoproteins bone sialoprotein and BAG-75, which are enriched within biomineralization foci, along with inhibiting activation of procollagen C proteinase enhancer protein. These results suggest that 105-kDa SKI-1 may be responsible for extracellular proteolytic processing of secreted proteins within biomineralization foci.

Because intracellular SKI-1 can also activate transmembrane transcription factor precursors, we carried out a whole genome array comparison of mineralizing *versus* AEBSF-treated cultures. Transcription of 140 genes was reduced by 1.5–3-fold including *Phex*, *Dmp1*, fibronectin, tenascin-N, tenascin-C, *COL11A1*, *COL1A1*, and *COL1A2*. This result was then validated when six of these genes were retested with a more specific inhibitor of SKI-1, dec-RRLL-cmk, using a quantitative PCR approach. Furthermore, treatment of primary cultures of transgenic DMP1-GFP calvarial cells with both SKI-1 inhibitors not only blocked mineralization but also inhibited GFP expression driven by a 10-kb DMP1 promoter. These findings demonstrate for the first time that both a general and a specific inhibitor of SKI-1 protease is able to coordinately block transcription of this group of mineralization-related genes. Because inactivation or deletion of the type XI collagen, type I collagen, *Dmp1*, or *Phex* gene *in vivo* either causes a bone deficiency phenotype or abnormal skeletal de-

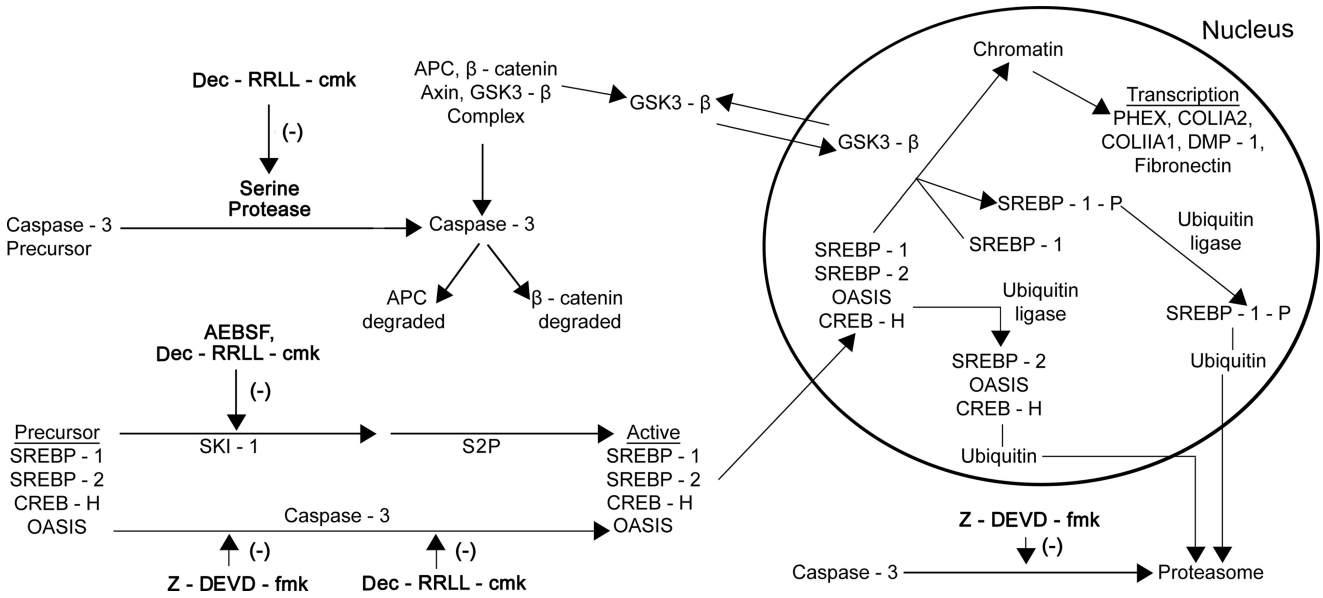

FIGURE 9. **Proposed intracellular mechanism of AEBSF, dec-RRLL-cmk, and Z-DEVD-fmk effects on gene expression by osteoblastic cells.** *Steps* depicted in *bold type* are those suggested from the experimental data presented here. Other parts of the model are derived from a variety of literature sources referenced under "Discussion." *GSK3*, glycogen synthase kinase-3. *APC*, adenomatous polyposis coli protein.

velopment (2–5, 7, 8, 47, 48), we propose that their combined reduced transcription is the primary mechanism by which AEBSF and dec-RRLL-cmk inhibit mineralization in osteoblastic cultures.

An additional unexpected stimulatory effect of dec-RRLL-cmk on transcription of COL1A2 suggests that type I collagen may not be required for initial mineral crystal nucleation and deposition within BMF in the UMR106-01 model. Rather, the blockage of procollagen C proteinase enhancer protein activation by AEBSF (16), which facilitates procollagen processing and fibril assembly, leads us to propose that type I collagen may function during subsequent propagation and growth of initial mineral crystals in this model. However, additional studies are needed to confirm that these transcriptional changes reflect differences in protein content.

Consideration of the effects of AEBSF and dec-RRLL-cmk on gene expression in osteoblastic cells immediately raises questions about whether the promoters for fibronectin, *DMP1*, *Phex*, *COL11A1*, and *COL1A2* are regulated by SKI-1-activated transcription factors. A review of the literature indicates that only the fibronectin and positive control HMG-CoA synthase promoters are known to be regulated by CREB and SREBP-2 (42, 43, 49, 50). However, ECR Browser searches of the proximal 5–6-kb promoters for the human, mouse, and rat fibronectin, *Dmp1*, *Phex*, *COL11A1*, HMG-CoA synthase, and *COL1A2* genes revealed conserved cyclic AMP response element and SRE consensus sequences in all six promoters (data not shown). Although these assignments do not ensure functionality, they are consistent with a common role for SKI-1 in regulating transcription of fibronectin, *Dmp1*, *Phex*, *COL11A1*, *COL1A2*, and HMG-CoA synthase.

Analysis of Nuclear Transcription Factor Content and Size Supports a Role for SKI-1 in Mineralization—The nuclear content of 58-kDa OASIS (CREB3L1) was decreased by AEBSF and dec-RRLL-cmk. These results are consistent with the known role of SKI-1 in activating OASIS. Furthermore, changes in the nuclear OASIS content brought about by AEBSF and dec-RRLL-cmk correlate well with changes both in the mineral content and the expression of COL11A1, FN, Phex, and Dmp-1 in osteoblastic cultures.

AEBSF and dec-RRLL-cmk each affected the nuclear contents of 68-kDa activated SREBP-1 and SREBP-2 differently. However, as expected, caspase-3-cleaved forms of SREBP-1 (58 kDa) and SREBP-2 (65 kDa) were enriched in +FBS cultures. We presume that the cause for this change is serum cholesterol inhibition mediated by SCAP (SREBP cleavage-activating protein) transport protein (41).

The response of SREBP-1 and SREBP-2 to Z-DEVD-fmk was also different. Although the rationale for this finding is not clear, we suggest that SREBP-1 could be activated by another caspase not susceptible to this inhibitor or that turnover of SREBP-1 and SREBP-2 may follow distinct pathways.

In summary, the nuclear contents of activated OASIS, SREBP-1, and SREBP-2 were all reduced in AEBSF- and dec-RRLL-cmk-treated cultures relative to mineralizing controls. Because the proximal promoters for fibronectin, COL11A1, Phex, and Dmp-1 all contain SRE consensus sequences (data not shown), our results suggest that these inhibitors mediate their effects in osteoblastic cells by blocking activation and nuclear import of these SKI-1-activated transcription factors leading to their diminished nuclear contents and reduced transcription of fibronectin, *COL11A1*, *Phex*, and *Dmp-1*.

Although fibronectin, COL11A1, Phex, and Dmp-1 responded uniformly to the presence of SKI-1 inhibitors, COL1A2 expression reacted oppositely and increased over controls in response to dec-RRLL-cmk. We speculate that regulation of COL1A2 expression may be more complex and that our results may reflect the actions of non-SKI-1-regulated transcription factors. However, it is interesting to note that despite an increase in COL1A2 expression, the overall

effect of dec-RRLL-cmk was to block mineralization in UMR106-01 cultures.

Effects of Inhibitors on Caspase-3 Activation and Caspase-3 Turnover—SREBP-1, SREBP-2, and CREB transcription factors all appear to be subject to proteasomal degradation (53, 54). Hirano *et al.* (53) showed that SREBP-1 is ubiquitinated and degraded in a manner consistent with the proteasome and that its 3-h half-life was increased when cells were treated with proteasome inhibitors. Interestingly, when ubiquitination was blocked, a small increase in nuclear SREBP-1 and SREBP-2 content was observed along with an increase in expression of HMG-CoA synthase. Three sites on SREBP-1 are important in terms of its phosphorylation (Thr-426 and Ser-430 and Ser-434). Interestingly, phosphorylation occurs after SREBP-1 binds to chromatin and is mediated by glycogen synthase kinase-3β (55, 56) (see the model in Fig. 9). Ubiquitin ligase Fbw7 is then recruited to SREBP-1-promoter complexes after its phosphorylation and catalyzes ubiquitinylation of lysines with subsequent proteasomal degradation of the modified SREBP-1. Based on this requirement and recent identification of its nuclear localization sequence (57), we have proposed that glycogen synthase kinase-3β can be imported into the nucleus (see the model in Fig. 9).

Because cytosolic caspase-3 can cleave adenomatous polyposis coli protein and β-catenin (58, 59), we speculate that a decrease in the intracellular content of activated caspase-3 could lead to an increase in cytosolic complexes of glycogen synthase kinase-3β with adenomatous polyposis coli protein and β-catenin (see the model in Fig. 9). In this way, less glycogen synthase kinase-3β would then be imported into the nucleus where it would phosphorylate SREBP-1 (and possibly SREBP-2 and OASIS), leading to their ultimate proteasomal degradation. Thus, when caspase-3 is inactivated by Z-DEVD-fmk or when activation of caspase-3 is inhibited by dec-RRLL-cmk, more glycogen synthase kinase-3β is predicted to remain complexed with axin, catenin, and adenomatous polyposis coli protein in the cytoplasm (60), unable to phosphorylate transcription factors and, thus, decreasing their turnover and transiently increasing their nuclear concentration. In a similar way, caspase inhibitors Z-VAD-fmk and Z-DEVD-fmk were shown to block apoptosis by suppressing NF-κB/p65 degradation, thereby increasing nuclear translocation, DNA binding, and transcriptional activity (61).

Direct Western blotting analyses demonstrated here that the level of the activated 19-kDa caspase-3 subunit was reduced in dec-RRLL-cmk-treated cultures. These findings are consistent with the report by Park *et al.* (62) who showed that a serine protease was required to activate caspase-3 during apoptosis initiated by TNF-α. These results suggest that SKI-1, a serine protease, can mediate directly or indirectly the activation of procaspase-3 (see the model in Fig. 9).

Although many studies have linked activation of SREBP-1 and SREBP-2 with endoplasmic reticulum stress and apoptosis (24), recent work has shown that SREBP activation is also a characteristic of differentiated cellular pathways such as membrane biogenesis associated with phagocytosis (63), the secretion of insulin by pancreatic beta cells (64), and the transcription of the low density lipoprotein receptor by endothelial cells induced by shear stress (65). Also, SREBP-1c (ADD-1) (66) is a major positive regulator of fatty acid synthesis in developing adipogenic tissues. Our results showing that SKI-1 inhibitors block mineralization and the coordinated transcription of key mineralization-related genes support a requirement for SKI-1 in the differentiation of osteoblastic cells. Prior evidence for a non-apoptotic role for caspase-3 in osteoblast differentiation was also presented by Mogi and Togari (52) and Miura *et al.* (51).

Our novel results demonstrate that a group of genes required for normal bone formation share a common transcriptional regulatory mechanism in mineralizing osteoblastic cells (see the model in Fig. 9). Comparative Western blot analyses of the sizes and contents of transcription factors SREBP-1, SREBP-2, OASIS, and CREB-H in AEBSF- or dec-RRLL-cmk-treated cultures further support the role of SKI-1 in the activation of these transcription factors, and, implicitly, in the regulation of *COL11A1*, *Phex*, *Dmp1*, and fibronectin. Careful analyses of the effects of these inhibitors also indicate a hierarchical relationship in which SKI-1 or another serine protease inhibited by dec-RRLL-cmk, but not by AEBSF, catalyzes the activation of caspase-3 in osteoblastic cells. Our results indicate that the differentiated phenotype of osteoblastic cells, and possibly osteocytes, depends upon the non-apoptotic actions of SKI-1 to regulate the synthesis of proteins (and lipids for vesicles) needed to assemble and mineralize the extracellular matrix of bone.

Acknowledgments—We acknowledge the valuable technical assistance provided by Ellen Henderson and Pat Veno and Adnan Cheema, who provided important graphics support. J. P. Gorski thanks the Bone Biology Group at University of Missouri-Kansas City for long term support on this project and Dr. Tim Osborne, University of California Irvine, for generous assistance in analysis of SKI-1-activated transcription factors. J. P. Gorski also thanks Dr. Kezhong Zhang, Wayne State University, for providing anti-CREB-H antiserum.

REFERENCES

1. Lian, J. B., and Stein, G. S. (1992) *Crit. Rev. Oral Biol. Med.* **3,** 269–305
2. Ruchon, A. F., Tenenhouse, H. S., Marcinkiewicz, M., Siegfried, G., Aubin, J. E., DesGroseillers, L., Crine, P., and Boileau, G. (2000) *J. Bone Miner. Res.* **15,** 1440–1450
3. The HYP Consortium (1995) *Nat. Genet.* **11,** 130–136
4. Lorenz-Depiereux, B., Bastepe, M., Benet-Pagès, A., Amyere, M., Wagenstaller, J., Müller-Barth, U., Badenhoop, K., Kaiser, S. M., Rittmaster, R. S., Shlossberg, A. H., Olivares, J. L., Loris, C., Ramos, F. J., Glorieux, F., Vikkula, M., Jüppner, H., and Strom, T. M. (2006) *Nat. Genet.* **38,** 1248–1250
5. Feng, J. Q., Ward, L. M., Liu, S., Lu, Y., Xie, Y., Yuan, B., Yu, X., Rauch, F., Davis, S. I., Zhang, S., Rios, H., Drezner, M. K., Quarles, L. D., Bonewald, L. F., and White, K. E. (2006) *Nat. Genet.* **38,** 1310–1315
6. Hansen, U., and Bruckner, P. (2003) *J. Biol. Chem.* **278,** 37352–37359
7. Li, Y., Lacerda, D. A., Warman, M. L., Beier, D. R., Yoshioka, H., Ninomiya, Y., Oxford, J. T., Morris, N. P., Andrikopoulos, K., and Ramirez, F. (1995) *Cell* **80,** 423–430
8. Richards, A. J., Yates, J. R., Williams, R., Payne, S. J., Pope, F. M., Scott, J. D., and Snead, M. P. (1996) *Hum. Mol. Genet.* **5,** 1339–1343
9. Schneider, G. B., Zaharias, R., and Stanford ,C. (2001) *J. Dent. Res.* **80,** 1540–1544
10. Moursi, A. M., Damsky, C. H., Lull, J., Zimmerman, D., Doty, S. B., Aota,

S., and Globus, R. K. (1996) *J. Cell Sci.* **109,** 1369–1380
11. Moursi, A. M., Globus, R. K., and Damsky, C. H. (1997) *J. Cell Sci.* **110,** 2187–2196
12. Stanford, C. M., Jacobson, P. A., Eanes, E. D., Lembke, L. A., and Midura, R. J. (1995) *J. Biol. Chem.* **270,** 9420–9428
13. Wang, A., Martin, J. A., Lembke, L. A., and Midura, R. J. (2000) *J. Biol. Chem.* **275,** 11082–11091
14. Gorski, J. P., Wang, A., Lovitch, D., Law, D., Powell, K., and Midura, R. J. (2004) *J. Biol. Chem.* **279,** 25455–25463
15. Midura, R. J., Wang, A., Lovitch, D., Law, D., Powell, K., and Gorski, J. P. (2004) J. *Biol. Chem.* **279,** 25464–25473
16. Huffman, N. T., Keightley, J. A., Chaoying, C., Midura, R. J., Lovitch, D., Veno, P. A., Dallas, S. L., and Gorski, J. P. (2007) *J. Biol. Chem.* **282,** 26002–26013
17. Wang, C., Wang, Y., Huffman, N. T., Cui, C., Yao, X., Midura, S., Midura, R. J., and Gorski, J. P. (2009) *J. Biol. Chem.* **284,** 7100–7113
18. Gorski, J. P., Huffman, N. T., Cui, C., Henderson, E. P., Midura, R. J., and Seidah, N. G. (2009) *Cells Tissues Organs* **189,** 25–32
19. Seidah, N. G., Mayer, G., Zaid, A., Rousselet, E., Nassoury, N., Poirier, S., Essalmani, R., and Prat, A. (2008) *Int. J. Biochem. Cell Biol.* **40,** 1111–1125
20. Wang, X., Pai, J. T., Wiedenfeld, E. A., Medina, J. C., Slaughter, C. A., Goldstein, J. L., and Brown, M. S. (1995) *J. Biol. Chem.* **270,** 18044–18050
21. Wang, X., Zelenski, N. G., Yang, J., Sakai, J., Brown, M. S., and Goldstein, J. L. (1996) *EMBO J.* **15,** 1012–1020
22. Higgins, M. E., and Ioannou, Y. A. (2001) *J. Lipid Res.* **42,** 1939–1946
23. Guan, G., Dai, P. H., Osborne, T. F., Kim, J. B., and Shechter, I. (1997) *J. Biol. Chem.* **272,** 10295–10302
24. Schröder, M. (2008) *Cell. Mol. Life Sci.* **65,** 862–894
25. Murakami, T., Kondo, S., Ogata, M., Kanemoto, S., Saito, A., Wanaka, A., and Imaizumi, K. (2006) *J. Neurochem.* **96,** 1090–1100
26. Murakami, T., Saito, A., Hino, S., Kondo, S., Kanemoto, S., Chihara, K., Sekiya, H., Tsumagari, K., Ochiai, K., Yoshinaga, K., Saitoh, M., Nishimura, R., Yoneda, T., Kou, I., Furuichi, T., Ikegawa, S., Ikawa, M., Okabe, M., Wanaka, A., and Imaizumi, K. (2009) *Nat. Cell Biol.* **11,** 1205–1211
27. Chandhoke, T. K., Huang, Y. F., Liu, F., Gronowicz, G. A., Adams, D. J., Harrison, J. R., and Kream, B. E. (2008) *Bone* **43,** 101–109
28. Schlombs, K., Wagner, T., and Scheel, J. (2003) *Proc. Natl. Acad. Sci. U.S.A.* **100,** 14024–14029
29. Patra, D., Xing, X., Davies, S., Bryan, J., Franz, C., Hunziker, E. B., and Sandell, L. J. (2007) *J. Cell Biol.* **179,** 687–700
30. Laemmli, U. K. (1970) *Nature* **227,** 680–685
31. Pullikotil, P., Vincent, M., Nichol, S. T., and Seidah, N. G. (2004) *J. Biol. Chem.* **279,** 17338–17347
32. Pullikotil, P., Benjannet, S., Mayne, J., and Seidah, N. G. (2007) *J. Biol. Chem.* **282,** 27402–27413
33. Zhang, K., Shen, X., Wu, J., Sakaki, K., Saunders, T., Rutkowski, D. T., Back, S. H., and Kaufman, R. J. (2006) *Cell* **124,** 587–599
34. Kalajzic, I., Braut, A., Guo, D., Jiang, X., Kronenberg, M. S., Mina, M., Harris, M. A., Harris, S. E., and Rowe, D. W. (2004) *Bone* **35,** 74–82
35. Kalajzic, I., Kalajzic, Z., Kaliterna, M., Gronowicz, G., Clark, S. H., Lichtler, A. C., and Rowe, D. (2002) *J. Bone Miner. Res.* **17,** 15–25
36. Kalajzic, I., Staal, A., Yang, W. P., Wu, Y., Johnson, S. E., Feyen, J. H., Krueger, W., Maye, P., Yu, F., Zhao, Y., Kuo, L., Gupta, R. R., Achenie, L. E., Wang, H. W., Shin, D. G., and Rowe, D. W. (2005) *J. Biol. Chem.* **280,** 24618–24626
37. Pasquato, A., Pullikotil, P., Asselin, M. C., Vacatello, M., Paolillo, L., Ghezzo, F., Basso, F., Di Bello, C., Dettin, M., and Seidah, N. G. (2006) *J. Biol. Chem.* **281,** 23471–23481
38. Seidah, N. G., Mowla, S. J., Hamelin, J., Mamarbachi, A. M., Benjannet, S., Touré, B. B., Basak, A., Munzer, J. S., Marcinkiewicz, J., Zhong, M., Barale, J. C., Lazure, C., Murphy, R. A., Chrétien, M., and Marcinkiewicz, M. (1999) *Proc. Natl. Acad. Sci. U.S.A.* **96,** 1321–1326
39. Elagoz, A., Benjannet, S., Mammarbassi, A., Wickham, L., and Seidah, N. G. (2002) *J. Biol. Chem.* **277,** 11265–11275
40. Henrich, S., Cameron, A., Bourenkov, G. P., Kiefersauer, R., Huber, R., Lindberg, I., Bode, W., and Than, M. E. (2003) *Nat. Struct. Biol.* **10,** 520–526
41. Nohturfft, A., Yabe, D., Goldstein, J. L., Brown, M. S., and Espenshade, P. J. (2000) *Cell* **102,** 315–323
42. Dooley, K. A., Bennett, M. K., and Osborne, T. F. (1999) *J. Biol. Chem.* **274,** 5285–5291
43. Inoue, J., Sato, R., and Maeda, M. (1998) *J Biochem.* **123,** 1191–1198
44. Chandler, J. M., Cohen, G. M., and MacFarlane, M. (1998) *J. Biol. Chem.* **273,** 10815–10818
45. Liu, X., Kim, C. N., Pohl, J., and Wang, X. (1996) *J. Biol. Chem.* **271,** 13371–13376
46. Omori, Y., Imai, J., Suzuki, Y., Watanabe, S., Tanigami, A., and Sugano, S. (2002) *Biochem. Biophys. Res. Commun.* **293,** 470–477
47. Dixon, P. H., Christie, P. T., Wooding, C., Trump, D., Grieff, M., Holm, I., Gertner, J. M., Schmidtke, J., Shah, B., Shaw, N., Smith, C., Tau, C., Schlessinger, D., Whyte, M. P., and Thakker, R. V. (1998) *J. Clin. Endocrinol. Metab.* **83,** 3615–3623
48. Pihlajaniemi, T., Dickson, L. A., Pope, F. M., Korhonen, V. R., Nicholls, A., Prockop, D. J., and Myers, J. C. (1984) *J Biol. Chem.* **259,** 12941–12944
49. Singh, L. P., Andy, J., Anyamale, V., Greene, K., Alexander, M., and Crook, E. D. (2001) *Diabetes* **50,** 2355–2362
50. Michaelson, J. E., Ritzenthaler, J. D., and Roman, J. (2002) *Am. J. Physiol. Lung Cell. Mol. Physiol.* **282,** L291–L301
51. Miura, M., Chen, X. D., Allen, M. R., Bi, Y., Gronthos, S., Seo, B. M., Lakhani, S., Flavell, R. A., Feng, X. H., Robey, P. G., Young, M., and Shi, S. (2004) *J. Clin. Invest.* **114,** 1704–1713
52. Mogi, M., and Togari, A. (2003) *J. Biol. Chem.* **278,** 47477–47482
53. Hirano, Y., Yoshida, M., Shimizu, M., and Sato, R. (2001) *J. Biol. Chem.* **276,** 36431–36437
54. Costes, S., Vandewalle, B., Tourrel-Cuzin, C., Broca, C., Linck, N., Bertrand, G., Kerr-Conte, J., Portha, B., Pattou, F., Bockaert, J., and Dalle, S. (2009) *Diabetes* **58,** 1105–1115
55. Punga, T., Bengoechea-Alonso, M. T., and Ericsson, J. (2006) *J. Biol. Chem.* **281,** 25278–25286
56. Bengoechea-Alonso, M. T., and Ericsson, J. (2009) *J. Biol. Chem.* **284,** 5885–5895
57. Meares, G. P., and Jope, R. S. (2007) *J. Biol. Chem.* **282,** 16989–17001
58. Webb, S. J., Nicholson, D., Bubb, V. J., and Wyllie, A. H. (1999) *FASEB J.* **13,** 339–346
59. Hunter, I., McGregor, D., and Robins, S. P. (2001) *J. Bone Miner. Res.* **16,** 466–477
60. Farr, G. H., 3rd, Ferkey, D. M., Yost, C., Pierce, S. B., Weaver, C., and Kimelman, D. (2000) *J. Cell Biol.* **148,** 691–702
61. Gupta, S., Hastak, K., Afaq, F., Ahmad, N., and Mukhtar, H. (2004) *Oncogene* **23,** 2507–2522
62. Park, I. C., Park, M. J., Choe, T. B., Jang, J. J., Hong, S. I., and Lee, S. H. (2000) *Int. J. Oncol.* **16,** 1243–1248
63. Castoreno, A. B., Wang, Y., Stockinger, W., Jarzylo, L. A., Du, H., Pagnon, J. C., Shieh, E. C., and Nohturfft, A. (2005) *Proc. Natl. Acad. Sci. U.S.A.* **102,** 13129–13134
64. Amemiya-Kudo, M., Oka, J., Ide, T., Matsuzaka, T., Sone, H., Yoshikawa, T., Yahagi, N., Ishibashi, S., Osuga, J., Yamada, N., Murase, T., and Shimano, H. (2005) *J. Biol. Chem.* **280,** 34577–34589
65. Liu, Y., Chen, B. P., Lu, M., Zhu, Y., Stemerman, M. B., Chien, S., and Shyy, J. Y. (2002) *Arterioscler. Thromb. Vasc. Biol.* **22,** 76–81
66. Gondret, F., Ferré, P., and Dugail, I. (2001) *J. Lipid Res.* **42,** 106–113

Gene Regulation:

Inhibition of Proprotein Convertase SKI-1 Blocks Transcription of Key Extracellular Matrix Genes Regulating Osteoblastic Mineralization

Jeff P. Gorski, Nichole T. Huffman, Sridar Chittur, Ronald J. Midura, Claudine Black, Julie Oxford and Nabil G. Seidah

J. Biol. Chem. 2011, 286:1836-1849.
doi: 10.1074/jbc.M110.151647 originally published online November 12, 2010
